Molecular dynamics simulations of dipolar fluids in orientationally ordered phases

Dong-Qing Wei,[1,*] Ying-Jie Wang,[1,2] Lu Wang,[1,2] Jin-He Hu,[1,2] Zi-Zheng Gong,[3] Yong-Xin Guo,[2] and Yi-Sheng Zhu[1]
[1]*College of Life Science and Biotechnology, Shanghai Jiaotong University, China 200240*
[2]*Physics Department, Liaoning University, Shenyang, China*
[3]*China Academy of Space Technology, Beijing, China*
(Received 8 November 2006; revised manuscript received 29 March 2007; published 6 June 2007)

It has been established that the strongly interacting dipoles form orientationally ordered liquid phases. However, most of the computer simulations adapt the point dipole model. In this paper, we report molecular dynamics simulations of orientationally order phases formed by extended dipoles, where the potential energy consists of the site-site Lennard-Jones potential and electrostatic contribution of partial charges. The calculations were performed for a range of densities along an isotherm and for different temperatures at the same reduced densities. It is found that orientationally ordered phases are present in the wide density regime, the extended dipole tends to form chains at low density, and the isotropic liquid phase is not seen in the density regime studied for a specific temperature.

DOI: 10.1103/PhysRevE.75.061702 PACS number(s): 64.70.Md, 61.25.Em, 61.20.Ja

I. INTRODUCTION

In recent years there has been renewed interest in the thermodynamic and structural properties of dipolar fluids, which consist of spherical particles with embedded point dipoles. In 1916, Born conjectured that dipolar forces alone can create an orientationally ordered fluid. In the early 1990s, the molecular dynamics (MD) simulations of Wei and Patey [1,3] for the model of soft spheres with electric point dipoles embedded at their centers represents the first contribution which shows that the dipolar interaction alone is capable of bringing about the formation of an orientationally ordered phase. Moreover, they showed that this phase is a ferroelectric liquid crystal, becoming a stable ferroelectric solid at high density. The Monte Carlo (MC) simulations of Weis *et al.* [4] for a system of strongly interacting dipolar hard spheres have revealed that dipolar hard spheres can also form an orientationally ordered phase. Levesque, Weis, and co-workers [5–8] also extended their previous MC calculations to lower densities and temperatures.

The systems of spheres with point dipoles are highly idealized ones. In order to search for the thermodynamic and molecular parameters that the ferroelectric liquid states are stable we have to consider more complex and more realistic systems. Ballenegger and Hansen [9] performed extensive MD simulations for systems of extended dipoles formed by two opposite charges $+/-q$ separated by a distance d (dipole moment $\mu=qd$) in the liquid state. The strengths and shortcomings of the point dipole model for polar fluids of spherical molecules are illustrated. The dependence of the pair structure, dielectric constant and dynamics on the charge separation is analyzed. However, the ferroelectric phase was not the focus of their studies. In 1997, Kachel and Gburski [10,11] performed MD simulations for a model system which consists of elongated molecules with three embedded interaction sites XY_2 placed on the major axis of the molecule. The sites *Y-X-Y* are responsible for the nondipolar intermolecular interaction of atomic groups (united atoms or pseudoatoms) located inside the molecule [8]. Their simulations have shown that the simple protoplasts of elongated molecules can form spatially ordered, chainlike structures. Subsequently, Patey *et al.* [12–14] considered fluids of hard spheres each carrying two parallel point dipoles using constant-volume Monte Carlo computer simulations, and the results show that both ferroelectric and antiferroelectric fluid phases can be stabilized at high density and low temperature by dipolar interactions alone, if the separation between the dipoles on each sphere was sufficiently large.

In the present paper, we performed MD simulations for a model system which consist of rigid polyatomic molecules with electric extended dipole; the dipole moment was along the prime axis in the molecular fixed frame. Our molecules have two effective charges q $\{0.5,-0.5\}$ located on the z axis (0.05 and −0.05 nm, respectively) and with the distance d =0.1 nm between them. In other words, the molecule has the dipole moment $\boldsymbol{\mu}$ ($\mu=|\boldsymbol{\mu}|=qd$, $q=0.5$). In the following sections, we shall describe the model, computational methods, and results.

II. COMPUTATIONAL METHODS

The model that we use is a common one for the rigid polyatomic molecules [15,16] where the intermolecular forces consist of short range Lennard-Jones (LJ) site-site forces combined with electrostatic long range forces. The potential energy for any two sites i,j is given by

$$U_{ij}(r) = \varepsilon_{ij}[(\sigma_{ij}/r)^{12} - (\sigma_{ij}/r_{ij})^{6}] + q_i q_j / r. \quad (1)$$

There are two sites (like diatomic molecule) on each molecule. ε_{ij} is the Lennard-Jones well depth and σ_{ij} is the distance at the Lennard-Jones minimum, q_i is the partial atomic charge, and r is the distance between atomic sites i and j, which belong to different molecules. The Lennard-Jones parameters between pairs of different atoms are obtained from the Lorentz-Berthelodt combination rules, in which ε_{ij} values are based on the geometric mean of ε_i and ε_j and σ_{ij} values are based on the arithmetic mean between σ_j and σ_j. The

*Corresponding author; dqwei@sjtu.edu.cn

long-range potential is treated by the Ewald sum method [14]. The equations of motion are solved using a quaternion leapfrog algorithm.

Our MD calculations were performed at constant temperature essentially as described by Kusalik [15]. We considered a model system of 256 particles in a cubic box with periodic boundary conditions. We used the cutoff radius $R^c = L/2$, where L is the length of the cubic simulation cell. The time step $\Delta t = 1$ fs was employed in all calculations. Typically, runs were begun with randomly oriented particles placed on a fcc lattice, and were equilibrated for about 50 000 time steps. Averages were then accumulated over at least another 100 000 time steps. However, much longer simulations were carried out in some selected densities in order to ensure that the equilibrium state was reached. The standard deviations were estimated by dividing the final 100 000 time steps into ten equal blocks and assuming for statistical purposes that the block averages constitute independent measurements of the physical properties of interest.

The LJ parameters are taken as $\varepsilon = 2.05 \times 10^{-21}$ J, $\sigma = 0.315$ nm, which is the same for all sites. The partial charges q $\{0.5, -0.5\}$ are placed on the z axis (0.05 and −0.05 nm); it gives a dipole moment of $8.0109 \times 10 - 30$ C m. To facilitate further discussion, the reduced units are defined: the LJ reduced temperature, $T^*_{LJ} = k_B T/\varepsilon_{LJ}$, where k_B is the Boltzmann constant; the LJ reduced dipole moment, $\mu^*_{LJ} = (\mu^2/\varepsilon_{LJ}\sigma^3)^{1/2} = 3$; the reduced density, $\rho^* = N\sigma^3/V$, where V is the volume and N is the number of particles. Simulations were carried out for a range of densities, $\rho^* = 0.19$–0.99 at a constant LJ reduced temperature $T^*_{LJ} = 2$. To gauge the effect of temperature we also performed simulation at a fixed density $\rho^* = 0.82$ for three LJ reduced temperatures i.e., $T^*_{LJ} = 2.0$, 2.67, and 3.35 (corresponding to $T = 297.1$, 397.1, and 497.1 K), respectively.

III. RESULTS AND DISCUSSION

The possible existence of an ordered phase was monitored by calculating the usual equilibrium first- and second-rank orientational order parameters, $\langle P_1 \rangle$ and $\langle P_2 \rangle$, respectively. For isotropic fluids both order parameters are zero. For ordinary nonferroelectric nematics $\langle P_2 \rangle \neq 0$, $\langle P_1 \rangle = 0$. For ferroelectric nematics both $\langle P_1 \rangle$ and $\langle P_2 \rangle$ must be nonzero. The instantaneous second-rank order parameter P_2 was taken to be the largest eigenvalue of the ordering matrix with the elements given by

$$Q_{\eta\xi} = N^{-1} \sum_{i=1}^{N} 2^{-1}(3 n_{i\eta} n_{i\xi} - \delta_{\eta\xi}), \tag{2}$$

where $n_{i\eta}$ is the η component of the unit vector $\mathbf{n}_i = \boldsymbol{\mu}_i/\mu_i$. The corresponding eigenvector is the instantaneous director $\mathbf{d}$, and the instantaneous first-rank order parameter P_1 is defined by

$$P_1 = N^{-1} \sum_{i=1}^{N} \mathbf{n}_i \cdot \mathbf{d}. \tag{3}$$

The equilibrium order parameters are the ensemble averages of P_1 and P_2.

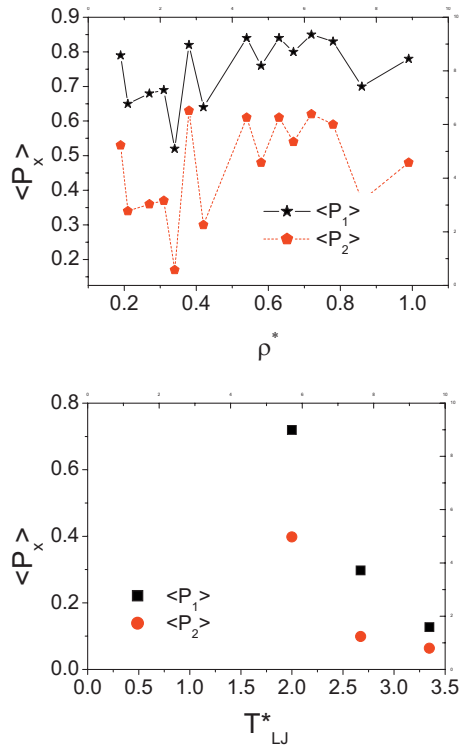

FIG. 1. (Color online) (a) The orientational order parameter as functions of reduced density. The simulations were performed at constant temperature $T^*_{LJ} = 2$ with 256 particles. The statistical deviations are estimated and smaller than the size of the symbols used. (b) The average order parameters as functions of temperature at $\rho^* = 0.82$. The statistical deviations are estimated and smaller than the size of the symbols used.

The order parameters as functions of reduced density are shown in Fig. 1(a). It can be seen that $\langle P_1 \rangle$ is significant even at small reduced density. However, $\langle P_2 \rangle$ fluctuates around 0.4. It is apparent that the ferroelectric phases are present in the whole density range. The dipoles form coiled chains in the low density regime: this explains partly why the value of $\langle P_1 \rangle$ and $\langle P_2 \rangle$ vary significantly when they are plotted as a function of density. When density goes higher the order parameter $\langle P_2 \rangle$ tends to converge to a higher value around 0.5. A large variation of the order parameters may also arise from underlying structure changes [5–8]. When the temperature increases it is expected that the chain formation would be less severe. This is confirmed in Fig. 1(b). We observe an isotropic liquid at $T^*_{LJ} = 3.35$ and $\rho^* = 0.82$.

In order to clearly distinguish fluid and solid phases, we have calculated the mean square displacement $\langle |r_i(t) - r_i(0)|^2 \rangle$, where r_i is the position of molecule i at time t; for fluids this quantity will continually increase with time varying linearly at long times according to the Einstein relationship [10] shown in Eq. (4),

$$2tD = \langle |r_i(t) - r_i(0)|^2 \rangle / 3, \tag{4}$$

where D is the diffusion coefficient. For solids the mean square displacement becomes constant rather than continually increasing with time. The mean square displacements

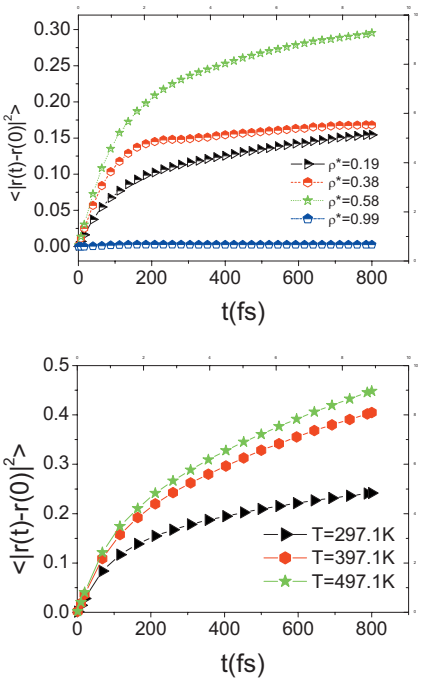

FIG. 2. (Color online) (a) The mean square displacement $\langle|r(t)-r(0)|^2\rangle$ as a function of time for a range of reduced densities at $T^*_{LJ}=2$ with 256 particles. The statistical deviations are estimated and smaller than the size of the symbols used. (b) The mean square displacement $\langle|r(t)-r(0)|^2\rangle$ as a function of time for different temperatures at $\rho^*=0.82$. The statistical deviations are estimated and smaller than the size of the symbols used.

were plotted in Fig. 2(a) and it was apparent that the system is fluid for the densities $\rho^*=0.19$, 0.38, 0.58, and at $\rho^*=0.99$ the quantity became constant and the system became solid. In Fig. 2(b) we observed that the mean square displacement is also affected by the temperature. Based on the results of mean square displacement, we find that the dipole system forms orientationally ordered liquid and solid phases, which is similar to the point dipole model except coiled chains are present in low density and the isotropic phase is not found at low temperature within the density regime studied. The solid phase is seen at $\rho^*=0.99$.

It is instructive to calculate the pair correlation function $g(r)$ to further understand the interactions between the dipoles. It is related to the probability of finding the center of a particle at a given distance from the center of another particle. For a many body system, one can write generally the correlation function in the following form:

$$\mathbf{g}(\mathbf{r}_1,\mathbf{r}_2,\ldots,\mathbf{r_n}) = \rho^n(\mathbf{1},\ldots,\mathbf{r_n})/\rho^n, \tag{5}$$

where $\rho^n(\mathbf{1},\ldots\mathbf{r_n})$ and ρ refer to the n body density profile and average density, respectively [17]. The simplest correlation function is the two-body correlation function of two specific sites on two molecules, for example, between site 1 of molecule 1 and site 2 of molecule 2, which is defined as

$$g_{12}(r) = N(N-1)\langle\delta(\mathbf{r}-\mathbf{r_1})\delta(\mathbf{r}-\mathbf{r_2})\rangle/\rho_0^2 \tag{6}$$

where $r=|\mathbf{r_1}-\mathbf{r_2}|$. When the distance between $\mathbf{r_1}$ and $\mathbf{r_2}$ is large enough the correlation disappears, so if $|\mathbf{r_1}-\mathbf{r_2}|\to\infty$,

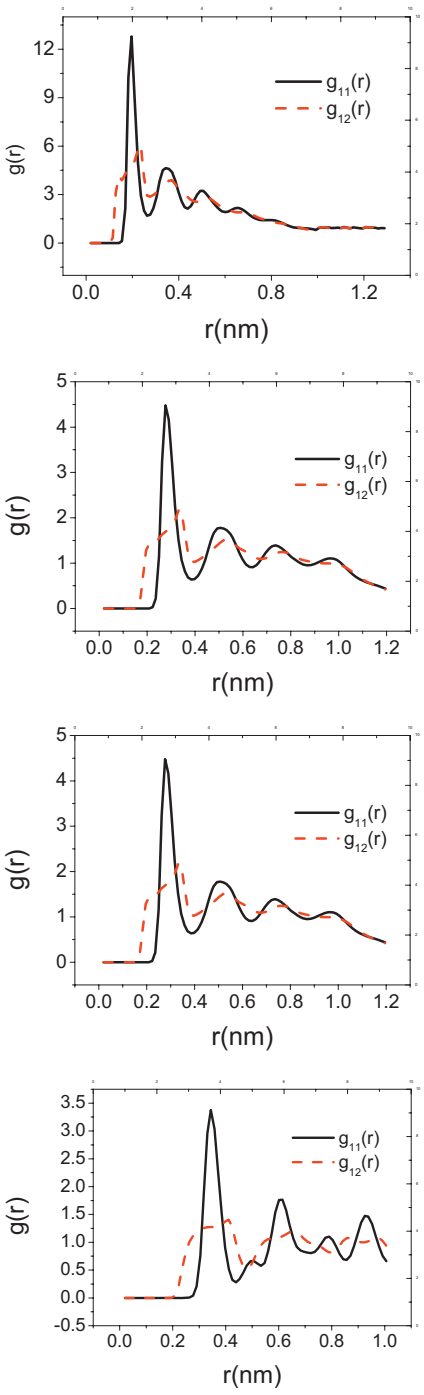

FIG. 3. (Color online) (a) The radial pair correlation function $g(r)$ as a function of r at $T^*_{LJ}=2$; for a law reduced density $\rho^*=0.19$. (b) The radial pair correlation function $g(r)$ as a function of r at $T^*_{LJ}=2$ for a reduced density $\rho^*=0.38$ in the liquid phase. (c) The radial pair correlation function $g(r)$ as a function of r at $T^*_{LJ}=2$ for a reduced density $\rho^*=0.58$. (d) The radial pair correlation function $g(r)$ as a function of r at $T^*_{LJ}=2$ for a reduced density $\rho^*=0.99$.

we expect $g(r)\to 1$. In general, for homogeneous systems in equilibrium, $g(r)$ should depend only on the relative position of the particles or the difference. The function $g(r)$ carries information on the structure of the system. For a crystal, it

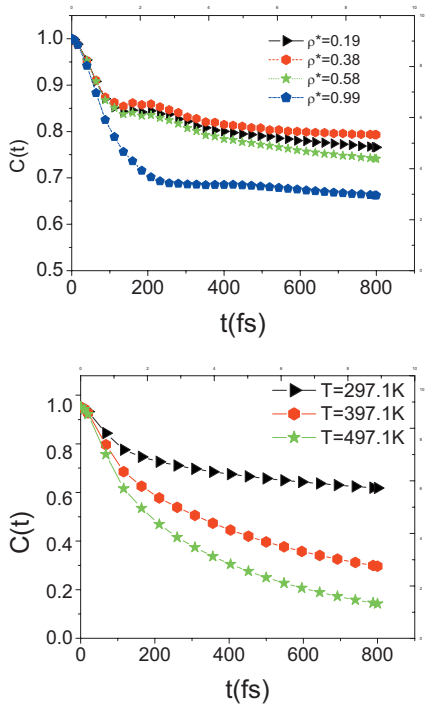

FIG. 4. (Color online) (a) The re-orientational correlation function $C(t)$ as a function of time at temperature $T^*_{LJ}=2$ for a range of reduced densities. (b) The re-orientational correlation function $C(t)$ as a function of time at reduced density $\rho^*=0.82$ for different temperatures.

exhibits a sequence of peaks at positions corresponding to shells around a given system. For amorphous materials and liquid, $g(r)$ exhibits its major peak close to the average atomic separation of neighboring atoms, and oscillates with less pronounced peaks at larger distances. The magnitude of the peaks usually decays exponentially with distance as $g(r)\rightarrow 1$. In most cases, $g(r)$ vanishes below a certain distance where atomic repulsion is strong enough to prevent pairs of atoms from getting too close.

We have calculated the radial distribution functions, which are shown in Fig. 3. One can see from Figs. 3(a) and 3(b) that the peaks of $g_{12}(r)$ are due to the correlation of positive and negative charges of two molecules within a chain where dipoles align head to tail. The sharp peak of $g_{11}(r)$ is due to the presence of neighboring chains which minimize the distance between the positive and negative charges of two separate chains. As a result, in the short range, chains are placed roughly in a body centered tetragonal (bct) structure [1,2]. In low density, the chain is less coiled as compares with the XY_2 model [7,8]. However, in the solid phase, the peak of $g_{11}(r)$ is pushed to a larger distance because the dipoles are placed on the bct lattice, all pointing in the same direction; sites 1 and 2 (positive-negative charges) are much closer to each other.

In addition to these structural properties, we have calculated the dipole-dipole re-orientational correlation function, which can be written in terms of the unit vector defined previously [18]:

$$C(t) = \sum_i \langle \mathbf{n_i}(0) \cdot \mathbf{n_i}(t) \rangle \Big/ \sum_i \langle \mathbf{n_i}(0) \cdot \mathbf{n_i}(0) \rangle .$$

It may help us understand the dynamics of dipoles in various phases. From Figs. 4(a) and 4(b) we see that $C(t)$ decays very slowly at the long time [18]. This is because the orientational correlation is long ranged in the ferroelectric order phases. However, $C(t)$ decayed sharply with increase of temperature, at $T^*_{LJ}=3.35$ ($T=497$) and the orientational order disappears which corresponds with the results of order parameter plots in Fig. 1(b).

IV. CONCLUSIONS

The ferroelectric phases are observed in all the density range studied at $T^*_{LJ}=2$ for the model system of extended dipoles. At a fixed density, i.e., $\rho^*=0.82$, the isotropic phase is seen at $T^*_{LJ}=3.35$. In the low density regime, some chains are formed which is rather similar to the point dipole model. When density goes higher the solid phase is found at $\rho^*=0.99$. For systems of point dipoles with the same reduced temperature and dipole moment, there is a well defined isotropic to ferroelectric liquid crystal phase transition, and no chain formation is found in low density. Given the importance and potential application of ferroelectric liquids it is worthwhile to pursue further studies of realistic polar liquids with strong polar interactions, which we are carrying out presently.

ACKNOWLEDGMENTS

D.Q.W. is very grateful for the referees whose comments have helped us greatly to shape the final version of this paper. This work was supported by grants from the Chinese National Science Foundation under Contract No. 10376024, and the Tianjin Commission of Education (Contract No. 20030001) and Tianjin Commission of Sciences and Technology under the Contract No. 033801911 and the special fund for intensive computation, and also the Virtual Laboratory for Computational Chemistry of CNIC and Supercomputing Center of CNIC, Chinese Academy of Sciences.

[1] D. Q. Wei and G. N. Patey, Phys. Rev. Lett. **68**, 2043 (1992).
[2] D. Q. Wei and G. N. Patey, Phys. Rev. A **46**, 7783 (1992).
[3] D. Q. Wei, G. N. Patey, and A. Perera, Phys. Rev. E **47**, 506 (1993).
[4] J. J. Weis, D. Levesque, and G. J. Zarragoicoechea, Phys. Rev. Lett. **69**, 913 (1992).
[5] D. Levesque and J. J. Weis, Phys. Rev. E **49**, 5131 (1994).
[6] J. J. Weis and D. Levesque, Phys. Rev. E **48**, 3728 (1993).
[7] J. J. Weis, J. Chem. Phys. **123**, 044503 (2005).
[8] J. M. Tavares, J. J. Weis, and M. M. Telo da Gama, Phys. Rev. E **73**, 041507 (2006).
[9] V. Ballenegger and J. P. Hansen, Mol. Phys. **102**, 599 (2004).

[10] A. Kachel and Z. Gburski, J. Mol. Spectrosc. **410**, 513 (1997).
[11] A. Kachel and Z. Gburski, J. Phys.: Condens. Matter **9**, 10095 (1997).
[12] V. V. Murashov, Philip J. Camp, and G. N. Patey, J. Chem. Phys. **116**, 6731 (2002). Philip J. Camp and G. N. Patey, Phys. Rev. E **60**, 4280 (1999).
[13] Philip J. Camp, J. C. Shelley, and G. N. Patey, Phys. Rev. Lett. **84**, 115 (2000).
[14] S. H. L. Klapp and G. N. Patey, J. Chem. Phys. **112**, 8 (2000).
[15] M. P. Allen and D. J. Tildesley, *Computer Simulation of Liquids* (Clarendon, Oxford, 1989) and references therein.
[16] P. G. Kusalik, J. Chem. Phys. **93**, 3520 (1990).
[17] J.-P. Hansen and I. R. McDonald, *Theory of Simple Liquids* (Academic Press Limited, London, 1990).
[18] D. Q. Wei and G. N. Patey, Phys. Rev. E **47**, 2954 (1993).